Additively manufactured Miura-Ori metamaterials with tailored design for energy absorption

Max Terrek Moester, Ava Ghalayaniesfahani, Daniel Saakes, Ian Gibson and Mehrshad Mehrpouya
Faculty of Engineering Technology, University of Twente, Enschede, The Netherlands

Abstract

Purpose – This study investigates Miura-Ori Metamaterials (MOMs), an origami-inspired class of mechanical metamaterials whose structural response is governed by folding geometry rather than material composition alone. The aim is to understand how variations in Miura-Ori unit-cell geometry influence compressive deformation behavior and energy dissipation capacity. By focusing on geometric effects, the study seeks to establish how MOM structures can be tailored to achieve desirable energy-absorbing performance while remaining lightweight and recoverable.

Design/methodology/approach – A parametric design model was developed in Grasshopper to generate Miura-Ori structures with adjustable geometric parameters. The Taguchi L9 design of experiments (DOE) method was applied to evaluate the influence of three key geometric parameters, wall thickness, dihedral angle and cell wall ratio, on the mechanical response. Samples were fabricated using fused filament fabrication (FFF) with thermoplastic polyurethane (TPU), selected for its flexibility and resilience. Mechanical characterization included tensile testing of the base material and quasi-static compression testing of the MOM samples. Stress–strain curves, onset densification strain, plateau stress and energy dissipation were calculated to assess overall performance.

Findings – The results demonstrate that the mechanical response of MOMs is highly sensitive to geometric configuration. Specific combinations of dihedral angle and cell wall ratio significantly improved the energy dissipation capacity. The findings indicate that MOMs can be systematically tuned to achieve desired levels of stiffness and energy absorption without altering material composition.

Originality/value – This work provides an experimentally validated framework for the geometry-driven optimization of MOMs. While the primary contribution centers on understanding fundamental mechanical behavior, the optimized structures can be further adapted for protective applications. As an example, the study proposes the potential integration of tuned MOM structures into custom-fit bicycle helmet liners.

Keywords Additive manufacturing, 3D printing, Metamaterial, Miura-Origami, Energy absorption

Paper type Research paper

1. Introduction

In recent years, Origami, the traditional Japanese art of paper folding, has evolved from an aesthetic practice into a powerful framework for engineering and scientific innovation. Origami structures are formed by folding two-dimensional sheets into ordered three-dimensional patterns, enabling lightweight, tunable and reversible architectures (Hu *et al.*, 2021; Mehrpouya *et al.*, 2022; Tachi, 2010; Xu *et al.*, 2023). Origami-inspired metamaterials have attracted growing attention as candidates for energy-absorbing systems (Krishnan *et al.*, 2022; Mehrpouya *et al.*, 2020; Mehrpouya and Huang, 2022; Mosleh *et al.*, 2017; Xiang *et al.*, 2020). Among the many tessellations, the Miura-Ori (MO) pattern has been studied extensively for its negative Poisson's ratio, high foldability and anisotropic response under loading. When extended into stacked configurations, the Miura-Ori Metamaterial (MOM) demonstrates excellent energy dissipation capabilities, making it particularly suitable for impact-mitigation applications.

While several geometric features can influence the mechanical response of MOMs, several studies indicate that not all parameters contribute equally. Wall thickness is consistently identified as a dominant factor due to its direct impact on structural stiffness and specific energy dissipation. The dihedral folding angle governs folding kinematics and compressive stiffness, where smaller angles often enhance energy dissipation by promoting progressive deformation. The cell wall ratio (a/b), as demonstrated by Zhang *et al.*, can significantly increase specific energy absoprtion compared to conventional honeycomb architectures (Zhang *et al.*, 2019). Additional factors, such as acute angle and stacking configuration, offer further tunability but with comparatively weaker influence. Hanna *et al.* and Harris *et al.* highlighted the sensitivity of energy dissipation to wall thickness and folding angle (Hanna *et al.*, 2021; Harris and

The current issue and full text archive of this journal is available on Emerald Insight at: **https://www.emerald.com/insight/1355-2546.htm**

Rapid Prototyping Journal
32/11 (2026) 63–72
Emerald Publishing Limited [ISSN 1355-2546]
[DOI 10.1108/RPJ-11-2025-0605]

Received 22 November 2025
Revised 3 March 2026
Accepted 22 March 2026

Rapid Prototyping Journal
Volume 32 · Number 11 · 2026 · 63–72

McShane, 2020), while Zhang *et al.* and Xiang *et al.* showed that variations in cell wall ratio and graded stacking can further enhance the performance of origami-inspired metamaterials (Xiang *et al.*, 2020; Zhang *et al.*, 2019).

Collectively, these studies confirm that the energy absorption behavior of MOM structures is governed primarily by geometric configuration rather than material type. However, despite the design flexibility afforded by origami-based geometries, the fabrication of MOMs has traditionally been constrained by manufacturing limitations, particularly in producing complex folded geometries with controlled wall thickness and repeatability. This constraint has limited the practical implementation of MOMs in functional components.

Additive manufacturing (AM) provides a fabrication route capable of overcoming the geometric limitations associated with conventional manufacturing methods. AM enables the layer-by-layer construction of complex three-dimensional geometries without the need for specialized tooling, making it particularly suitable for architected mechanical metamaterials (Ghalayaniesfahani *et al.*, 2024; Mehrpouya *et al.*, 2022; Wu *et al.*, 2019; Zadpoor, 2016). Among AM techniques, fused filament fabrication (FFF) provides an accessible and effective method for fabricating such structures, as it allows precise control over wall thickness, internal architecture, infill pattern and local material stiffness (M Mehrpouya, 2023; Zolfagharian *et al.*, 2025). This ability to directly tune geometry during fabrication is especially valuable when designing metamaterials whose mechanical response is governed by structural configuration, including multi-stable, deployable or auxetic lattice systems (Llanos *et al.*, 2025). To realize such controlled deformation behavior, the choice of printing material is critical. Thermoplastic polyurethane (TPU) is selected as the printing material due to its combination of flexibility, resilience and intrinsic damping capacity. Unlike brittle polymers commonly used in FFF, TPU can undergo large elastic deformations and recover its original shape, making it suitable for structures designed to absorb and release mechanical energy (Ursini and Collini, 2021; Xu *et al.*, 2020). Previous studies have demonstrated that TPU-based lattice structures exhibit stable compressive response, low permanent deformation and enhanced energy dissipation under repeated loading (Beloshenko *et al.*, 2021; Sood *et al.*, 2024). These characteristics make TPU particularly well suited for MOMs, where reversible folding and controlled deformation are essential to achieving tunable energy dissipation behavior.

This study systematically investigates how geometric configuration influences the mechanical behavior of MOMs. A parametric MO modeling workflow was developed to vary unit-cell geometry while preserving kinematic compatibility. The mechanical performance of the structures was examined with a focus on three key geometric parameters previously identified as most influential to energy dissipation: wall thickness (t), dihedral angle (θ) and cell wall ratio (a/b). Wall thickness governs stiffness and load-bearing capacity, the dihedral angle controls folding mechanics and deformation mode, and the cell wall ratio affects strain distribution within the unit cell. To efficiently evaluate the effects and interactions of these parameters, the Taguchi method was employed. Finally, the resulting insights were applied to the integration of MOMs into customizable impact-protection components, with a prototype bicycle helmet liner developed as a demonstration example.

2. Materials and characterization

2.1 Materials and printing

TPU filament was used as the base material for the FFF process in this study. Two commercial grades, TPU 85A (NinjaFlex 85A, NinjaTek, USA) and TPU 95A (NinjaFlex 95A, NinjaTek, USA), were initially selected to evaluate the influence of material stiffness and ductility on the deformation behavior of MOMs. These two grades differ primarily in Shore hardness, with TPU 85A being softer and more flexible, while TPU 95A exhibits higher stiffness and strength. Since energy-absorbing lattice structures require a balance between flexibility, recoverability and load-bearing capacity, a preliminary material screening was conducted to determine the most suitable grade for MOM fabrication. Their corresponding printing parameters are listed in Table 1.

Both materials were processed using a FFF 3D printer (Creality 3D Technology, China) equipped with a direct-drive extruder (BondTech, Sweden) and a 0.4 mm nozzle. The printing parameters were a nozzle temperature of 235°C, a bed temperature of 40°C, a print speed of 20 mm/s and a retraction distance of 3.6 mm.

2.2 Miura-Ori design and geometry

The superior energy-absorbing behavior of MOMs arises from their geometrical configuration as illustrated in Figure 1, which is governed by multiple interdependent parameters that strongly influence the resulting mechanical performance Table 2.

The geometry of MOMs shown in Figure 2 is composed of two complementary MO sheets, commonly referred to as sheet A and sheet B, tessellated in the X– and Y–directions and stacked in the Z–direction to form a cellular assembly. A typical configuration follows an "ABABA" stacking sequence (Schenk and Guest, 2013). Stacking is only achievable when geometric compatibility between adjacent sheets is satisfied, requiring equal crease lengths (SA = SB, VA = VB, LA = LB) and a thickness condition (HB > HA) to maintain foldability through the entire deformation process.

In particular, Xiang *et al.* examined the effect of folding geometry on the compressive behavior of MOMs by varying the acute angle (α) and introducing both uniform and graded stacking configurations in nylon-based specimens fabricated via polymer additive manufacturing (Xiang *et al.*, 2020). Their

Table 1 Printing parameters of TPU 85A and TPU95A

Material	Printing temperature [°C]	Printing speed [mm/s]	Build plate temperature [°C]	Infill density [%]
TPU85A Ninja Flex 85A	225–250	15–35	50	50
TPU 95A	220–240	15–35	30–60	50

Figure 1 Overview of the geometrical parameters of the Miura-Ori unit cell

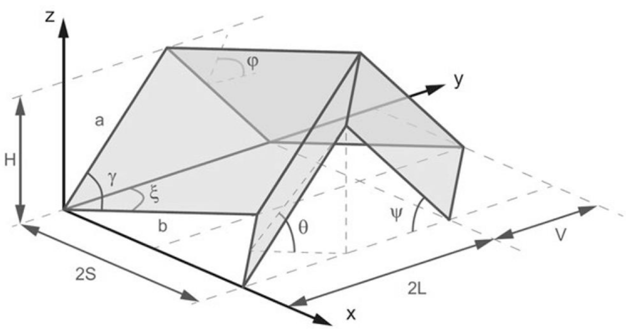

Source: adopted from Schenk and Guest (2013)

Table 2 Geometrical parameters of a Miura-Ori unit cell

Parameter	Symbol
Cell wall length	a
Cell wall length	b
Dihedral angle 1	ψ
Dihedral angle 2	ϕ
Folding angle 1	ξ
Folding angle 2	θ
Parallelogram angle	γ
Cell wall thickness	t
Cell wall ratio	a/b

results showed that energy absorption was highest when α ranged from 50° to 55°, and that graded stacking configurations exhibited substantially better performance than uniform assemblies. Zhang *et al.* compared MOM structures with conventional honeycomb cores under quasi-static compression and demonstrated that increasing the cell wall ratio (a/b) significantly enhanced the energy absorption, enabling MOMs to outperform traditional honeycomb architectures (Zhang *et al.*, 2019). Lv *et al.* examined the effects of wall thickness (t), dihedral angle (θ) and acute angle (α) on the deformation behavior of MO patterned sheets (Lv *et al.*, 2019). They reported that increasing wall thickness or decreasing the dihedral angle improved energy absorption and stiffness, while adjusting the acute angle influenced the peak force response.

The MOM structure is constructed from alternating sheet A and sheet B, tessellated in the X–Y plane and stacked in the Z-direction. Compatibility between the two sheets requires geometric constraints to be satisfied, but within these limits, the unit cell can be defined by multiple parameters, such as wall thickness, dihedral angle, folding angle, acute angle and the ratio of adjacent cell walls (a/b). Not all parameters are equally important. Literature shows that wall thickness strongly affects load-bearing capacity and energy dissipation, dihedral angle influences folding mechanics and compressive stiffness, and the cell wall ratio (a/b) significantly improves dissipated energy. These three parameters were therefore selected for systematic investigation in this study.

To generate and adjust the MO geometries, a parametric model was developed in Grasshopper (Rhinoceros 3D, USA). This model provided direct control over the key geometric parameters of the unit cell, allowing wall thickness, dihedral angle and cell wall ratio to be varied independently while preserving the intended fold pattern. Grasshopper also enabled the tessellation of the unit cell into larger stacked configurations without introducing geometric distortion. The accuracy of the parametric model was verified by comparing its output to established MO reference geometries, with deviations maintained within 5%, ensuring that the digital designs reliably represented the physical samples produced for testing Figure 3.

2.3 Design of experiment

A full factorial investigation of these three factors at three levels each would require 27 experimental runs. When multiplied by

Figure 2 Schematic illustration of the construction of Miura-Ori sheets A and B, after which they are stacked according to the stacking sequence: ABABA

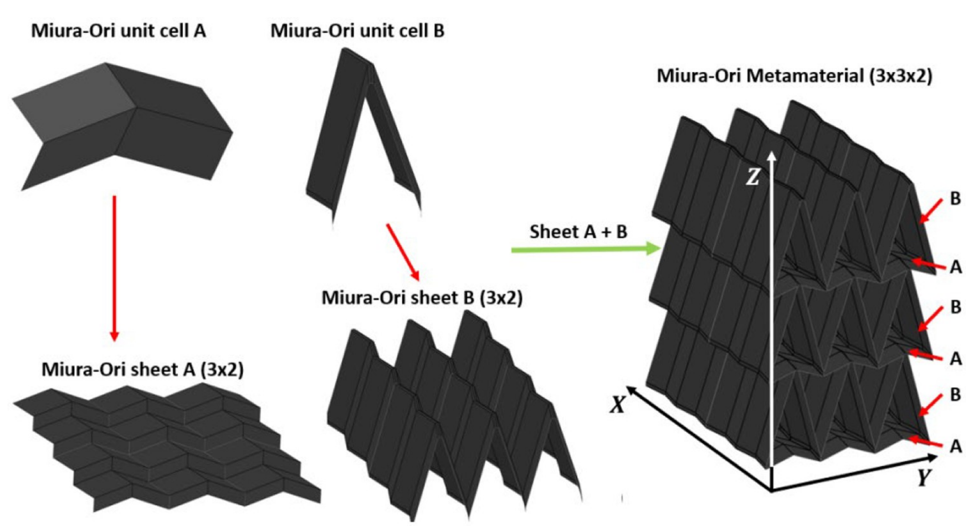

Figure 3 Schematic overview of the digital modeling process to generate the MOM structure

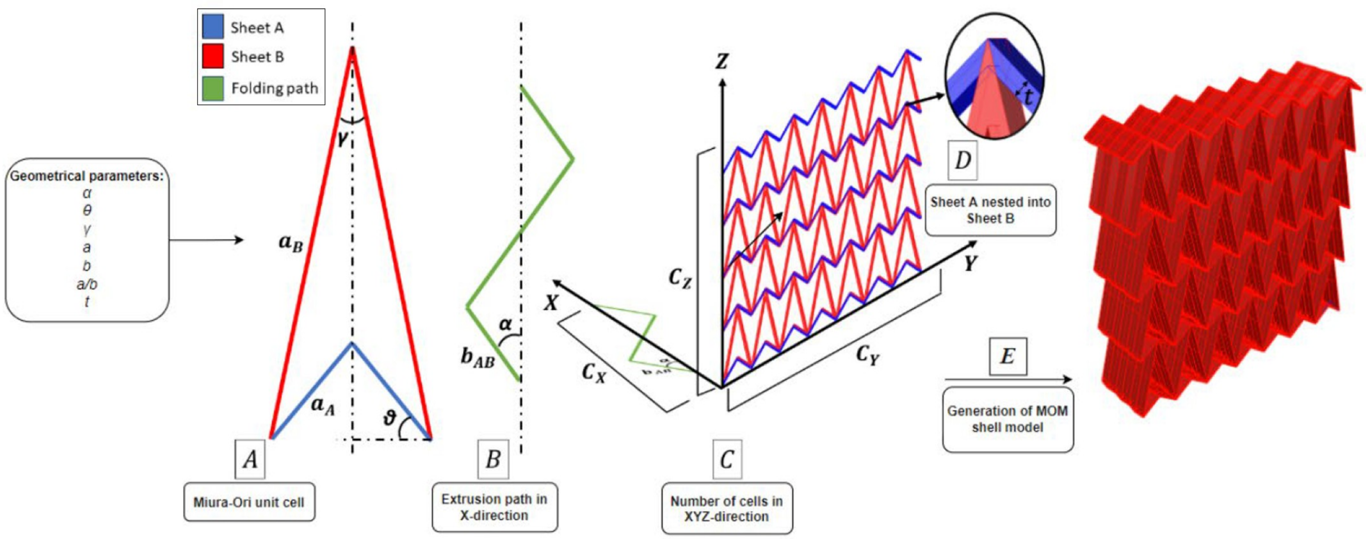

repetitions to ensure statistical reliability, such an approach would result in a substantial experimental workload in terms of fabrication time and material consumption. To efficiently analyze the effects of the selected geometric parameters while minimizing the number of experiments, the Taguchi design of experiments (DOE) method was adopted using Minitab software (version 20; Minitab, LLC, USA).

The Taguchi method is widely used in engineering optimization because it employs orthogonal arrays to systematically evaluate multiple control factors with a reduced number of experiments, while maintaining balanced representation of factor levels. In addition to reducing experimental effort, this approach improves robustness by separating the influence of control variables from experimental noise. Performance evaluation is carried out using signal-to-noise (S/N) ratios, which quantify the sensitivity of the response variable to variability, and analysis of variance (ANOVA), which determines the statistical significance and percentage contribution of each factor to the overall response (Hanna *et al.*, 2021; Islam and Pramanik, 2016).

In this study, an L9 orthogonal array was selected to evaluate three geometric parameters at three levels each, reducing the number of required trials from 27 to nine while still enabling systematic analysis of factor effects. The "larger-the-better" S/N ratio criterion was applied, since the objective was to maximize energy dissipation. ANOVA was subsequently performed to quantify the relative contribution and statistical significance of each parameter. The selected parameter levels were guided by both literature and manufacturing feasibility. For wall thickness, levels were set at 0.4 mm, 0.7 mm and 1.0 mm, with the lower bound constrained by the printer nozzle diameter and the upper bound by structural compatibility. For the dihedral angle, levels of 20°, 35° and 50° were chosen, with 20° identified in prior studies as a promising lower limit. For the cell wall ratio (a/b), levels of 1.5, 2.0 and 2.5 were selected, following the findings of (Lv *et al.*, 2019), which demonstrated improved energy absorption with increasing ratios.

Since variations in geometric parameters inherently alter the material fraction of the lattice, the relative density $\left(\frac{\rho^*}{\rho_s}\right)$ of each specimen was calculated from the computer-aided design (CAD) models. Relative density was defined as the ratio between the solid volume of the MO structure (V_{solid}) and the external bounding box volume ($V_{external}$):

$$\frac{\rho^*}{\rho_s} = \frac{V_{solid}}{V_{external}}$$

All samples shared identical external dimensions (54,000 mm^3), ensuring that differences in relative density were solely governed by geometric configuration. The geometric parameters used in the Taguchi design are summarized in Table 3. All nine samples, each with different geometric parameters and numbers of unit cells, were successfully 3D-printed in accordance with the deviation limits defined in Grasshopper, as shown in Figure 4.

2.4 Mechanical testing

Tensile properties of TPU85A and TPU95A were evaluated to support material selection. Tests were conducted according to ISO 37:2017 using Type II dumbbell-shaped specimens. The specimens were fabricated using optimized FFF parameters. Testing was performed using a universal testing machine (model Z 5.0, ZwickRoell, The Netherlands) equipped with hydraulic clamps set at 4.0 bar pressure. The stress-elongation behavior was recorded, and key mechanical parameters, tensile strength, elongation at break and elastic modulus, were extracted from the data.

To evaluate the energy dissipation performance of the MOM structures, quasi-static out-of-plane compression tests were also performed at room temperature using a universal testing machine (model Z 5.0, ZwickRoell, The Netherlands) equipped with a 5 kN load cell. Specimens were compressed between two flat plates at a constant crosshead speed of 2mm/min until a strain of 53.3% was reached, ensuring that all samples entered the densification region. After reaching this limit, the force was unloaded. Figure 5 shows the sample position in the compression test.

Table 3 Orthogonal array L9 of geometrical parameters for taguchi's method

Sample	Wall thickness (mm)	Dihedral angle (°)	Cell wall ratio (a/b)	Relative density (%)
1	0.4	20	1.5	13.48
2	0.4	35	2.0	13.11
3	0.4	50	2.5	16.48
4	0.7	20	2.0	18.82
5	0.7	35	2.5	22.82
6	0.7	50	1.5	31.52
7	1.0	20	2.5	24.46
8	1.0	35	1.5	39.65
9	1.0	50	2.0	36.93

Figure 4 Nine 3D printed MOM structures based on the DOE of this study

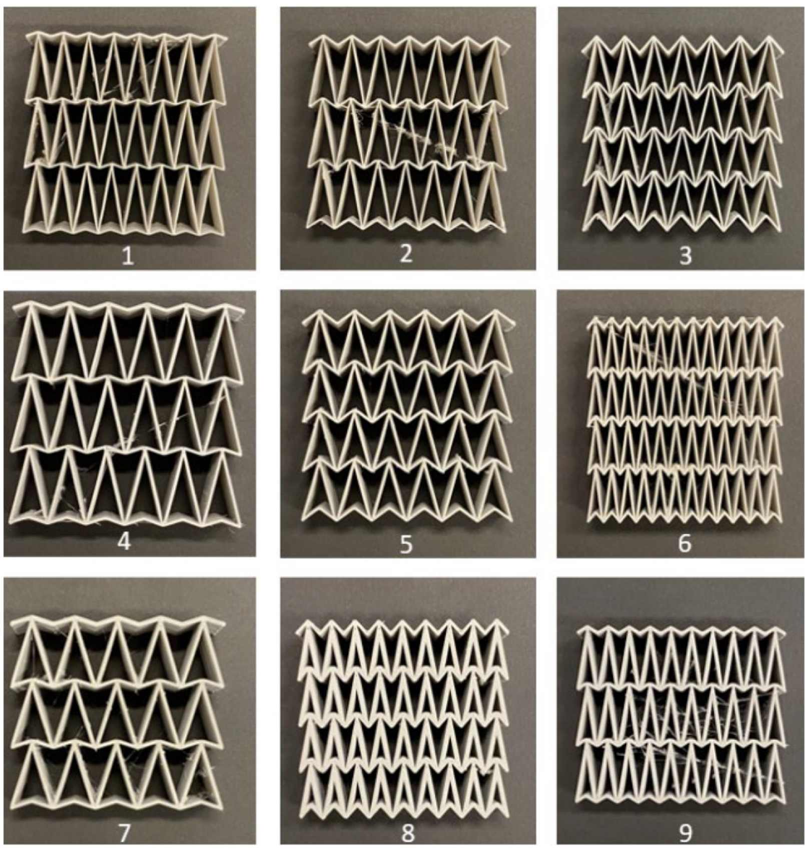

Force–displacement data were used to calculate energy dissipation. Each sample was tested in triplicate to verify repeatability of the mechanical response. The tests exhibited consistent force–displacement profiles with negligible qualitative variation. The area under the loading curve represents the total mechanical energy absorbed by the structure during compression, including both elastic and inelastic contributions. The area under the unloading curve corresponds to the recoverable elastic energy stored in the structure. The difference between these two areas defines the dissipated energy, which represents the portion of energy irreversibly lost due to internal friction, material damping and structural instabilities. The dissipated energy was calculated from the force–displacement data using the following equations:

$$Dissipated\ \ Energy = Stored\ \ Energy - Released\ \ Energy$$
$$= \int_0^{\delta_d} F\,d\delta - \int_{\delta_d}^{0} F\,d\delta \quad (1)$$

Equation (1) is employed to calculate the dissipated energy from the difference between the stored energy during loading and the released energy during unloading, where δ_{d} represents the maximum length of the stroke during the quasi-static compression test, and F denotes the compression force of displacement.

Figure 5 Loading direction of the printed sample in the compression test

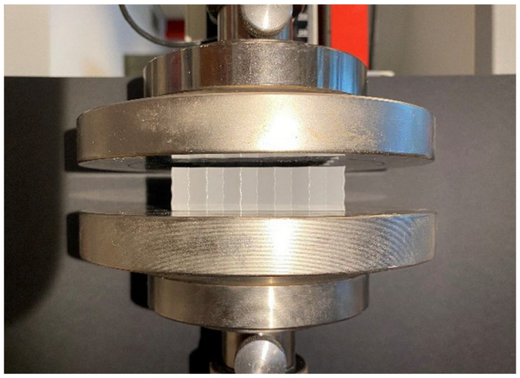

3. Results and discussion

3.1 Tensile testing results

The tensile behavior of both filaments was evaluated to determine their suitability for energy-absorbing lattice structures. The results indicated that TPU85A exhibited significantly higher elongation at break and more ductile behavior compared to TPU95A. TPU85A achieved an elongation of up to 540%, compared to approximately 320% for TPU95A, with a lower Young's modulus, making it ideal for flexible and recoverable deformation under load. This superior flexibility of TPU85A was critical for absorbing energy during compression, as it allowed the printed lattices to undergo large deformations without permanent damage Table 4.

3.2 Quasi-Static compression

Quasi-static compression tests were conducted on various MOM designs, and the force–displacement (F–D) data were analyzed to extract the energy absorption (EA). The averages of the test results for all nine samples are plotted in Figure 6, showing a wide range of force responses. The applied compression strain of 53.3% (i.e. 8 mm displacement) ensured that all samples reached the densification region, allowing the EA and its efficiency to be determined.

To better visualize individual F–D curves, the samples were grouped according to wall thickness. The results for samples with a wall thickness of 0.4 mm are shown in Figure 6(a). All samples exhibited similar inflection points, initial slopes and peak forces. Interestingly, sample 1 showed a higher peak force (210 N) prior to the plateau, whereas samples 2 and 3 had similar peak forces of 183 N. Sample 1 also exhibited a more

Table 4 Material properties of TPU 85A and TPU 95A 3D printed samples obtained by the tensile tests

Material	TPU 85A	TPU 95A
Young's modulus [MPa]	13.98	25.3
Ult. Tensile strength [MPa]	30.69	21.66
Elongation [%]	681.51	404.54

Figure 6 Force–displacement curves of all nine samples, presented in three separate plots corresponding to different wall thicknesses. Each plot includes both loading and unloading directions: (a) t = 0.4 mm (samples 1–3), (b) t = 0.7 mm (samples 4–6), and (c) t = 1.0 mm (samples 7–9)

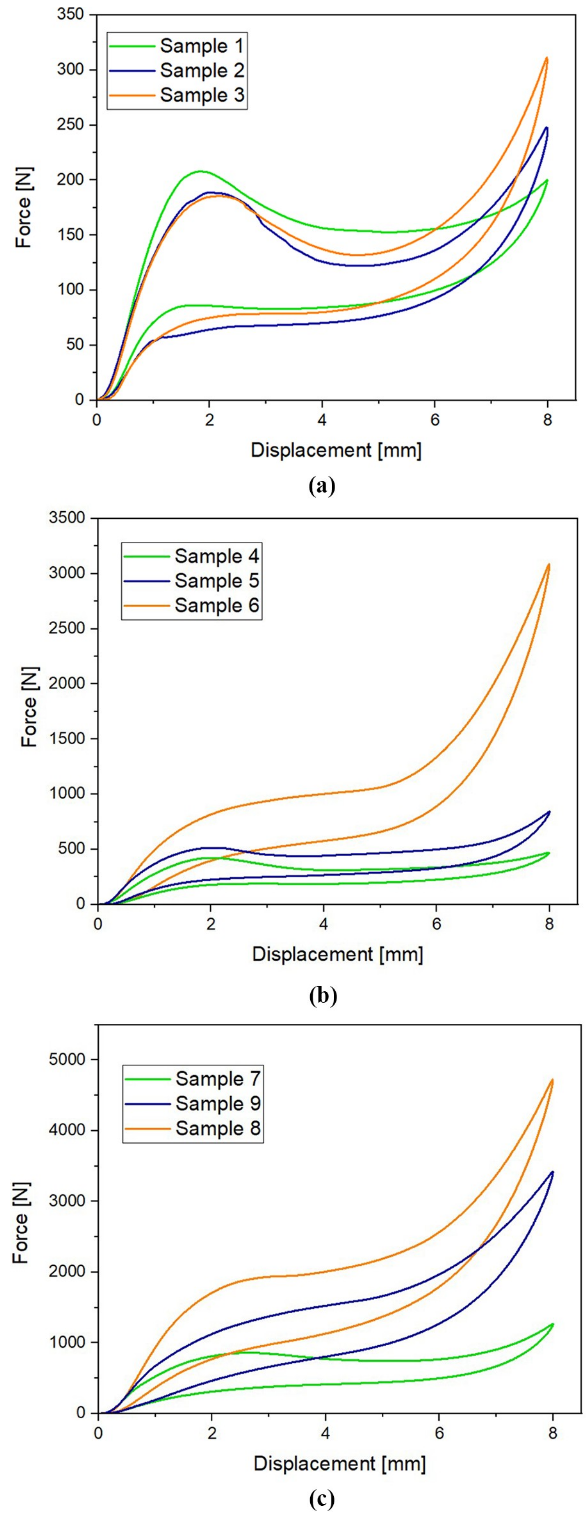

Rapid Prototyping Journal
Volume 32 · Number 11 · 2026 · 63–72

quasi-rectangular profile, with a smaller force drop and a longer plateau region.

In Figure 6(b), the samples with a wall thickness of 0.7 mm are presented. Sample 6 did not show a clear inflection point or distinct peak force, while samples 4 and 5 displayed similar peak forces and quasi-rectangular profiles. Sample 6 exhibited characteristics of a quasi-linear profile (Robinson *et al.*, 2017), with a higher peak force and a higher but shorter plateau force compared to samples 4 and 5. Sample 6 reached the densification region at approximately 5.5 mm, whereas samples 4 and 5 densified around 6–7 mm.

Finally, Figure 6(c) shows the samples with a wall thickness of 1.0 mm. Sample 9 did not display a clearly visible inflection point or plateau force, and, similar to sample 6, exhibited a quasi-linear profile. These two samples (6 and 9) had more gradual loading curves with very short or almost no plateau regions and transitioned almost directly into densification.

Figure 7 The maximum applied force and the dissipated energy of all 9 samples

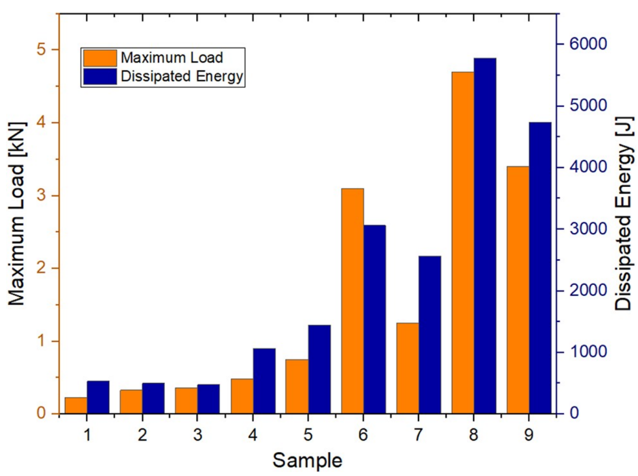

Distinct peak forces of 850 and 1950 N were recorded for samples 7 and 8, respectively. Sample 7 exhibited a plateau force similar to samples 1 and 4, again showing quasi-rectangular profiles.

It is noteworthy that samples 1, 4 and 7 all had the same dihedral angle of 20° but differed in wall thickness, cell wall ratio (CWR) and relative density. Their plateau forces had similar lengths prior to densification, indicating that a lower dihedral angle contributes to a longer plateau region, consistent with observations by Hanna *et al.* (2021). In addition, samples 1, 6 and 8 had a CWR of 1.5, and all exhibited higher initial slopes and peak forces compared to samples with CWRs of 2.0 or 2.5. Overall, the F–D curves indicate that a lower dihedral angle results in a longer plateau before densification. Increasing wall thickness led to higher peak and plateau forces, whereas increasing CWR caused a decrease in both peak and plateau forces.

Figure 7 shows the maximum load and energy absorption for all samples. As illustrated, sample 8 exhibited the highest compressive strength (4.7 kN), followed by sample 9 (3.6 kN) and sample 6 (3.3 kN). A similar trend was observed for dissipated energy, with sample 8 achieving the highest value of 57 kJ.

3.3 Effect of design parameters

A detailed parametric study revealed the influence of several geometric parameters on energy dissipation. Increasing the number of Miura cells in the lattice enhanced the deformation capacity and energy dissipation up to an optimal point. A greater inclination angle promoted distributed buckling and resulted in higher energy dissipation. Moreover, a minimum wall thickness of 0.4 mm was necessary to maintain structural integrity during both printing and testing. Lattices with excessive overhang angles exhibited poor print quality and premature failure, highlighting the importance of considering manufacturability in the design process.

Figure 8 Effect of geometrical parameters (wall thickness, dihedral angle and cell wall ratio) on energy dissipation by ANOVA analysis

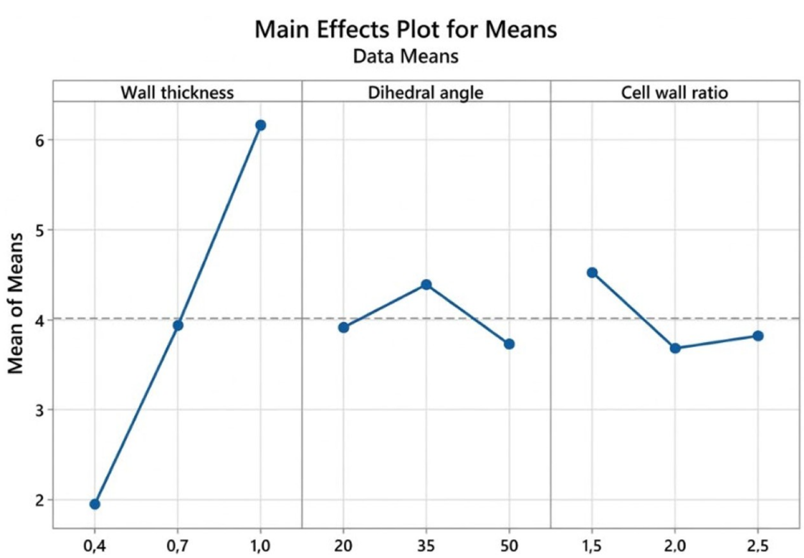

Figure 9 Workflow for creating the custom-fit Miura–Ori helmet liner. (a) 3D scanning of the human head and export to STL; the helmet liner is divided into multiple surfaces, and the axes are unified. (b) Initial result of the surface morph showing the volume available for the MOM structures

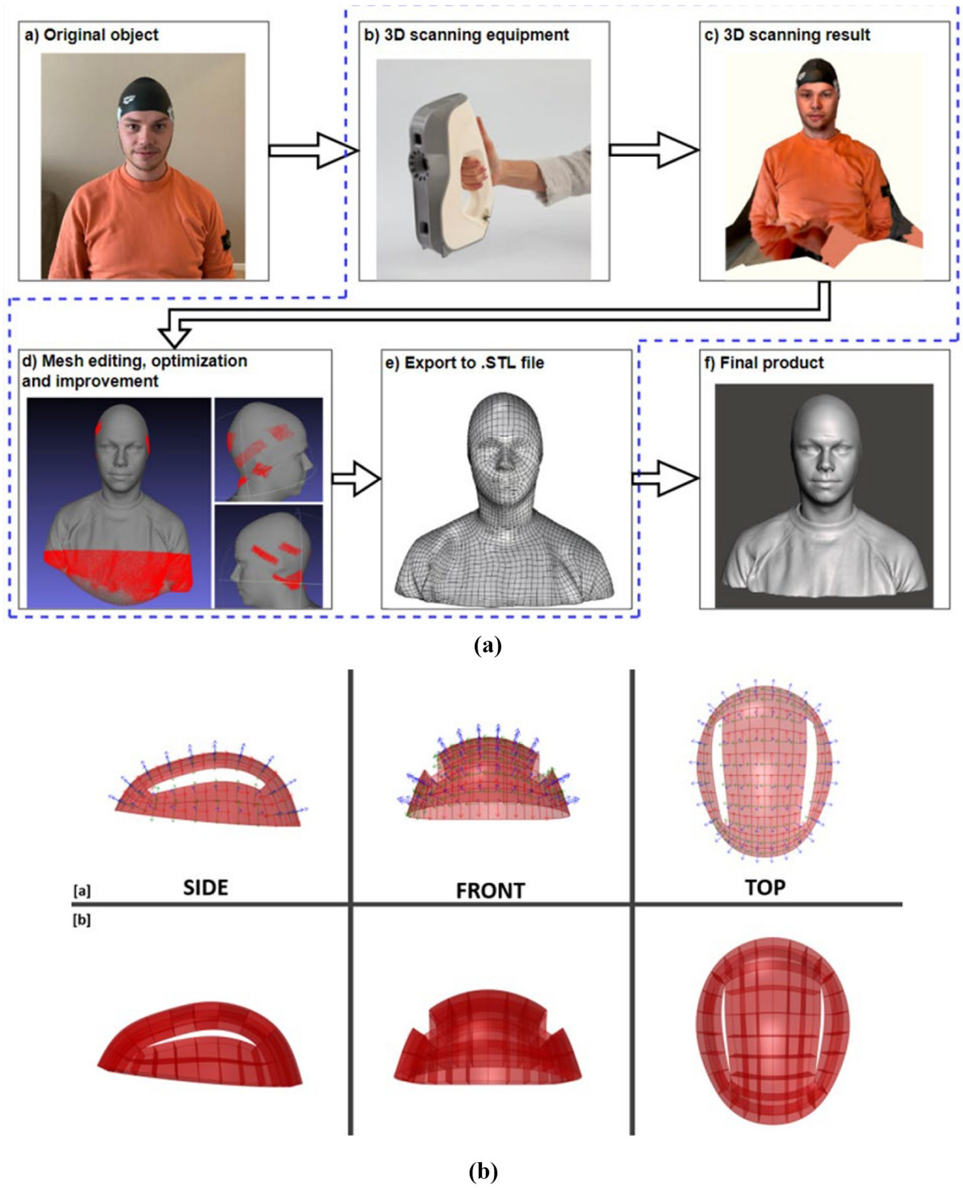

The main effects shown in Figure 8 and the ANOVA analysis confirmed that wall thickness had the most significant effect on energy dissipation, followed by the dihedral angle. In addition to individual effects, interaction effects between the geometric parameters were evaluated using the Taguchi method. The analysis revealed that the interaction between wall thickness and dihedral angle had a noticeable influence on energy dissipation: at higher wall thicknesses, variations in dihedral angle resulted in more pronounced changes in energy absorption. Interactions involving cell wall ratio were less significant but still contributed to subtle variations in deformation behavior. These findings indicate that optimal energy dissipation is governed not only by individual parameter levels but also by their combined interactions.

It is important to recognize that variations in wall thickness and cell wall ratio significantly modify the relative density of the MO structures, which ranged from 13.1% to 39.7%. As expected for cellular materials, higher relative density generally resulted in increased peak force and greater total absorbed energy. Notably, sample 8, which exhibited the highest energy dissipation, also possessed the highest relative density (39.65%). However, the ANOVA results indicate that wall thickness remains the statistically dominant parameter influencing performance. While relative density scales the magnitude of the load-bearing response, geometric parameters such as dihedral angle govern deformation mode and plateau characteristics. Therefore, the observed trends cannot be attributed solely to density variation, but rather to the combined influence of density scaling and geometry-controlled deformation mechanisms.

3.4 Final prototyping

To demonstrate the practical applicability of the optimized MOM, a custom-fit bicycle helmet liner was developed as a proof-of-concept application. This prototype was intended to illustrate the feasibility of integrating geometry-tuned metamaterials into wearable protective systems, rather than to provide a validated assessment of impact protection performance.

Although expanded polystyrene (EPS) and polyurethane foam (PUF) are the most commonly used materials for such applications due to their lightweight nature and cost-effectiveness, they permanently deform after a single impact and are produced in standardized sizes that do not accommodate the wide variety of human head shapes (Siegkas *et al.*, 2019; Thai *et al.*, 2015). These limitations have motivated the development of a new liner concept that combines improved energy dissipation with a customized fit. In our previous study, a comparison between PUF and 3D-printed TPU was conducted, demonstrating that 3D-printed TPU provides a more versatile and effective solution than traditional foam materials such as PUF (Zolfagharian *et al.*, 2025).

For this prototype, the wearer's head geometry was captured using a multi-angle 3D scanning process, generating a high-resolution digital head model. The steps from scanning to the final CAD model are illustrated in Figure 9(a). This model was imported into a parametric design environment, enabling the MO liner to be precisely fitted to the inner contour of the helmet shell [see Figure 9(b)]. The liner was fabricated using FFF printing with TPU, while the outer shell was produced in Polylactic acid.

The prototype consisted of five individually printed parts, as shown in Figure 10(a). The top part was the heaviest, and the front part was the lightest [Figure 10(b)]. The numerical weight was calculated using Rhinoceros, resulting in a total of 142 g, while the actual measured weight was 150.9 g. The close agreement between numerical and actual weights indicates that the printing parameters were well optimized. The prototype maintained dimensional accuracy, with no observable warping or print defects, demonstrating that the manufacturing workflow is reproducible and suitable for custom mass-personalization [see Figure 10(c)]. This demonstration highlights the potential of MOMs for integration into protective equipment, where conformal fit, tunable energy dissipation and lightweight performance are essential.

4. Conclusion

This study investigated the energy dissipation behavior of MOM structures fabricated via FFF using TPU. A parametric modeling framework was developed in Grasshopper to systematically vary key geometric features, focusing on wall thickness, dihedral angle and cell wall ratio, which were identified in prior research as the most influential parameters for mechanical response.

The results demonstrated that wall thickness is the dominant factor affecting specific energy dissipation, accounting for approximately 95% of the performance variance, while dihedral angle and cell wall ratio had smaller but measurable effects. Increasing wall thickness enhanced total absorbed energy but reduced energy dissipation efficiency due to earlier densification. Optimal performance was achieved with a wall thickness of 1.0 mm, a dihedral angle of 35° and a cell wall ratio of 1.5, yielding a maximum dissipated energy of 57 kJ (sample 8).

These findings confirm that the mechanical response of MOM structures can be effectively tuned through geometry alone, highlighting their potential as adaptable energy-absorbing metamaterials. While this study focused on quasi-static compression behavior, the strain-rate sensitivity of TPU suggests that higher peak forces and energy absorption may occur under dynamic loading. Although the absolute response is expected to change, the geometry-driven trends identified in this work are anticipated to remain valid. Future research will therefore investigate high strain-rate and impact loading conditions to fully assess the suitability of MOMs for real-world protective applications.

Acknowledgements

The authors gratefully acknowledge the support received from *Mr. Bert Vos* for the support in providing the mechanical testing equipment for this study.

Figure 10 Final additively manufactured bicycle helmet prototype, (a) The five individually 3D-printed MOM structures for placement in the outer shell, (b) The 3D-printed outer shell from PLA, (c) The fully assembled helmet with the MOM structures integrated into the outer shell

(a) (b) (c)

References

Beloshenko, V., Beygelzimer, Y., Chishko, V., Savchenko, B., Sova, N., Verbylo, D., ... Vozniak, I. (2021), "Mechanical properties of flexible TPU-based 3d printed lattice structures: role of lattice cut direction and architecture", *Polymers*, Vol. 13 No. 17, p. 2986.

Ghalayaniesfahani, A., Oostenbrink, B., van Kasteren, H., Gibson, I. and Mehrpouya, M. (2024), "4D printing of biobased shape memory sandwich structures", *Polymer*, Vol. 307, p. 127252.

Hanna, B., Adams, R., Townsend, S., Robinson, M., Soe, S., Stewart, M., ... Theobald, P. (2021), "Auxetic metamaterial optimisation for head impact mitigation in American football", *International Journal of Impact Engineering*, Vol. 157, p. 103991.

Harris, J. and McShane, G. (2020), "Metallic stacked origami cellular materials: additive manufacturing, properties, and modelling", *International Journal of Solids and Structures*, Vol. 185-186, pp. 448-466.

Hu, Y., Zhou, Y. and Liang, H. (2021), "Constructing rigid-foldable generalized miura-ori tessellations for curved surfaces", *Journal of Mechanisms and Robotics*, Vol. 13 No. 1, p. 11017.

Islam, M.N. and Pramanik, A. (2016), "Comparison of design of experiments via traditional and taguchi method", *Journal of Advanced Manufacturing Systems*, Vol. 15 No. 3, pp. 151-160.

Krishnan, B.R., Biswas, A.N., Kumar, K.A. and Sreekanth, P.R. (2022), "Auxetic structure metamaterial for crash safety of sports helmet", *Materials Today: Proceedings*, Vol. 56, pp. 1043-1049.

Llanos, C.M., Saakes, D. and Mehrpouya, M. (2025), "Additive manufacturing of adaptive architected structures for enhanced protective equipment", *European Journal of Mechanics - A/Solids*, Vol. 112, p. 105649.

Lv, Y., Zhang, Y., Gong, N., Li, Z-X., Lu, G. and Xiang, X. (2019), "On the out-of-plane compression of a miura-ori patterned sheet", *International Journal of Mechanical Sciences*, Vols 161-162, p. 105022.

M Mehrpouya, H.V. (2023), "Additive manufacturing of biopolymers: handbook of materials", *Techniques, and Applications*, Vol. 1, Elsevier.

Mehrpouya, M. and Huang, W.M. (2022), "Origami-inspired 4D printing", *Smart Materials in Additive Manufacturing*, Elsevier, pp. 373-394.

Mehrpouya, M., Azizi, A., Janbaz, S. and Gisario, A. (2020), "Investigation on the functionality of thermoresponsive origami structures", *Advanced Engineering Materials*, Vol. 22 No. 8, p. 2000296.

Mehrpouya, M., Edelijn, T., Ibrahim, M., Mohebshahedin, A., Gisario, A. and Barletta, M. (2022), "Functional behavior and energy absorption characteristics of additively manufactured smart sandwich structures", *Advanced Engineering Materials*, Vol. 24 No. 9, p. 2200677.

Mosleh, Y., Vander Sloten, J., Depreitere, B. and Ivens, J. (2017), "Novel composite foam concept for head protection in oblique impacts", *Advanced Engineering Materials*, Vol. 19 No. 10, p. 1700059.

Robinson, M., Soe, S., McShane, G., Celeghini, R., Burek, R., Alves, M. and Theobald, P. (2017), "Developing elastomeric cellular structures for multiple head impacts".

Schenk, M. and Guest, S.D. (2013), "Geometry of miura-folded metamaterials", *Proceedings of the National Academy of Sciences*, Vol. 110 No. 9, pp. 3276-3281.

Siegkas, P., Sharp, D.J. and Ghajari, M. (2019), "The traumatic brain injury mitigation effects of a new viscoelastic add-on liner", *Scientific Reports*, Vol. 9 No. 1, p. 3471.

Sood, M., Wu, C.-M. and Yang, Y.-C. (2024), "Mechanical properties of 3D-printed lattice cylindrical structure with recyclable elastomeric and thermoplastic polymers", *Journal of Polymers and the Environment*, Vol. 32 No. 9, pp. 4196-4212.

Tachi, T. (2010), "Geometric considerations for the design of rigid origami structures", Paper presented at the Proceedings of the International Association for Shell and Spatial Structures (IASS) Symposium.

Thai, K.T., McIntosh, A.S. and Pang, T.Y. (2015), "Factors affecting motorcycle helmet use: size selection, stability, and position", *Traffic Injury Prevention*, Vol. 16 No. 3, pp. 276-282.

Ursini, C. and Collini, L. (2021), "FDM layering deposition effects on mechanical response of TPU lattice structures", *Materials*, Vol. 14 No. 19, p. 5645.

Wu, X., Su, Y. and Shi, J. (2019), "Perspective of additive manufacturing for metamaterials development", *Smart Materials and Structures*, Vol. 28 No. 9, p. 93001.

Xiang, X., Lu, G. and You, Z. (2020), "Energy absorption of origami inspired structures and materials", *Thin-Walled Structures*, Vol. 157, p. 107130.

Xu, T., Shen, W., Lin, X. and Xie, Y.M. (2020), "Mechanical properties of additively manufactured thermoplastic polyurethane (TPU) material affected by various processing parameters", *Polymers*, Vol. 12 No. 12, p. 3010.

Xu, W., Huang, Y., Li, H., Luo, Y. and Wu, Y. (2023), "Research on mechanical properties and impact resistance of origami-based metamaterial for GIL", *Frontiers in Materials*, Vol. 10, p. 1208510.

Zadpoor, A.A. (2016), "Mechanical meta-materials", *Materials Horizons*, Vol. 3 No. 5, pp. 371-381.

Zhang, J., Karagiozova, D., You, Z., Chen, Y. and Lu, G. (2019), "Quasi-static large deformation compressive behaviour of origami-based metamaterials", *International Journal of Mechanical Sciences*, Vols 153-154, pp. 194-207.

Zolfagharian, A., Català, G.B., Saakes, D., Rolfe, B., Gibson, I. and Mehrpouya, M. (2025), "3D-printed architected material for the generation of foam-based protective equipment", *Advanced Engineering Materials*, Vol. 27 No. 21, p. 2500132.

Corresponding author

Mehrshad Mehrpouya can be contacted at: m.mehrpouya@utwente.nl